Journal of Energy

VOLUME 69 Number 1 | 2020

journal homepage: http://journalofenergy.com/

**Antonijo Kunac**

**Marin Despalatović**

**Dario Šantić**

Department of Electrical Engineering
FESB
University of Split
Croatia

# Synchrophasors Determination Based on Interpolated FFT Algorithm

## SUMMARY

Within the standard IEEE C37.118 applications and proposed hardware structure of a phasor measurement unit (PMU) are described. This paper presents the concept of the system for measuring and transferring synchrophasors from a theoretical aspect. Synchrophasor algorithms are developed in MATLAB/Simulink for the purpose of easier verification and hardware deployment on today's market available and affordable real time development kits. Analysis of the synchrophasor measurement process is performed gradually. Firstly, by defining the synchrophasor based on three-phase to $\alpha\beta$-transformation and then introducing a discrete Fourier transform (DFT) based on synchrophasor estimation algorithm. Later, accompanying adverse effects resulting from its application are analyzed by means of simulation. To increase accuracy and improve estimation algorithm interpolated discrete Fourier transform (IpDFT) with and without windowing technique is used. To further optimize algorithm performance convolution sum in recursive form has been implemented instead of classical DFT approach. This study was carried out in order to validate described measurement system for the monitoring of transients during island operation of a local power electric system. Finally, simulation and experimental results including error analysis are also presented.

## KEYWORDS

Digital signal processing, Discrete Fourier transforms, Modeling, Phasor measurement unit, Simulation

## INTRODUCTION

The development of information and communication technology has provided preconditions for automatization of the electric power system. Moreover, significant progress in managing and controlling the operation of the complete system as well as improving the quality and reliability of the electricity supply have also been achieved.

The classic approach used to manage and monitor electric power system is the supervisory control and data acquisition (SCADA) system. It is a system whose upgrades has reached their limits and are not so ''open'' to the latest technology. Therefore, intensive work on developing new remote management systems based on smart grid solutions is still ongoing process. Remote control and monitoring systems play a major role in determining optimal solutions for failures in electrical power systems, which significantly reduces investment and maintenance costs, as well as reducing losses due to interruptions and undelivered electricity. The quality of electricity is determined by the following parameters: voltage quality, supply reliability and service quality. Because of the increasingly stringent requirements for electricity quality, intelligent electronic device (IED) development is indispensable. Some of IEDs used for this purpose are: remote terminal unit (RTU), digital multimeters, power quality (PQ) monitors, etc.

Currently, the latest and most promising version of the IED is a phasor measurement unit (PMU). PMU represent a technology that has enabled insight into the real-time (RT) electrical power system dynamics [1], [2]. In this paper PMU algorithms for synchrophasor estimation are developed in MATLAB/Simulink.

The main task of the algorithm is to estimate parameters of the fundamental tone of the signal (amplitude, frequency and phase) [3]. Discrete Fourier transform (DFT) is the most commonly used method for identifying the fundamental tone of the signal [4], [5]. Generally, the advantages of the DFT approach are low computational complexity and harmonic rejection, while the drawbacks are spectral leakage and aliasing. In this paper to counteract these effects Fourier analysis and interpolated discrete Fourier transform (IpDFT) have been used [6]. This algorithm combined with and without use of windowing technique as well as use of convolution sum in recursive form will be described in the following sections.

# DIGITAL SIGNAL PROCESSING

### DFT algorithms

Main steps when applying a DFT-based digital signal processing technique to a continuous signal *x*(*t*) are shown in Fig. 1.

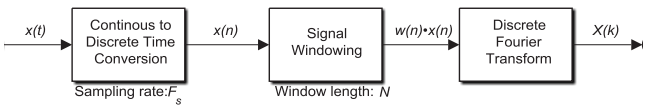


Block diagram of digital signal processing [3].

The Fourier transform (FT) of a continuous time-function *x*(*t*) is defined as follows

$$X(f) = \int_{-\infty}^{\infty} x(t) \cdot \mathrm{e}^{-\mathrm{j}2\pi ft}\, dt \tag{1}$$

As can be seen, FT is used to transform a continuous time-domain function *x*(*t*) to a continuous frequency-domain function *X*(*f*). In order to implement signal processing algorithms into a digital system, conversion of an analog signal to its digital representation must be performed [3].

Therefore, the discrete-time FT (DTFT) allows a transformation of a discrete sequence of infinite length *x*(*n*) into a continuous frequency-domain function

$$X(f) = \sum_{n=-\infty}^{\infty} x(n) \cdot \mathrm{e}^{-\mathrm{j}2\pi fn} \tag{2}$$

Since upper expression is continuous and infinite it is not appropriate for digital signal processing and cannot be applied for real-time applications. The discrete Fourier series (DFS) is another way to transform an infinite continuous periodic sequence in the frequency domain. When the DFS is used to transform a generic discrete periodic finite-length sequence of samples, it is called the DFT [8].

### Scalar to vector representation of three-phase system

For the sake of simplification, we assume balanced three-phase system of instantaneous voltages

$$\begin{aligned} v_a &= A(t) \cdot \cos(\phi(t)) \\ v_b &= A(t) \cdot \cos(\phi(t) - 2\pi/3) \\ v_c &= A(t) \cdot \cos(\phi(t) + 2\pi/3) \end{aligned} \tag{3}$$

where *A*(*t*) is the arbitrary magnitude function of time, while phase angle function may be expressed as

$$\phi(t) = 2\pi \int_0 f(t)dt + \phi(0) \tag{4}$$

where (0) is the initial phase angle value, and *f*(*t*) is the arbitrary frequency function of time. For the purpose of following analysis, we assume

$$f(t) = f_o + \Delta F \cdot \cos \Omega t \tag{5}$$

where *fo* is the average grid frequency assumed to be equal to 50 Hz, Δ*F* is the peak value of frequency deviation, and Ω is the angular modulation frequency of the fundamental harmonic *fo*, respectively. If (5) is inserted in (4), assuming zero phase initial value and after simplification, we obtain

$$\phi(t) = 2\pi f_o t + \frac{\Delta F}{\Omega} \cdot \sin \Omega t \tag{6}$$

Since balanced three-phase system is assumed, it is convenient to apply $\alpha\beta$-transformation on *abc* variables, which is equal to reduction of three to two-phase system [9]. Also known as the Clarke transformation, after applying it to scalar representation (3) the following complex voltage time function, i.e. synchrophasor, may be written

$$v(t) = v_\alpha(t) + \mathrm{j}\, v_\beta(t) \tag{7}$$

where the real and imaginary parts on the right-hand side of equation correspond to the transformed $\alpha$ and $\beta$ voltage components, respectively. Instead of using rectangular coordinate system in (7) for the ease of analysis more appropriate is polar coordinate system that gives

$$v(t) = A(t) \cdot \mathrm{e}^{-\mathrm{j}\phi(t)} \tag{8}$$

Thus, one should observe that for the three-phase system $\alpha\beta$-transformation is equal to the Hilbert's transform for single phase system. In other words, any real signal can be transformed using Hilbert's transform into a so-called analytical signal [8]. Additionally, (8) is equivalent to the reference signal used for space vector modulation control of three-phase inverters [9], [10].

### Discretization of continuous time signals

A discrete-time signal of (8), produced by a sampling process characterized with the sampling period *Ts*, is

$$v[n] = A[n] \cdot \exp\left(\mathrm{j}2\pi\left(f_o n T_s + \left(\Delta F / \Omega\right) \cdot \sin\left(\Omega n T_s\right)\right)\right) \tag{9}$$

where $0 \le n \le N\text{-}1$ is the sample number, and *N* is the total number of observed samples. Hence, the input signal is sliced in blocks containing *N* samples.

DFT of the observed signal is calculated in discrete points $k = 0, \ldots, N\text{-}1$ according to the following expression

$$V[k] = \sum_{n=0}^{N-1} v[n] \cdot \mathrm{e}^{-\mathrm{j}\frac{2\pi k}{N} n} \tag{10}$$

For the case of pure sinusoidal three-phase system with fundamental period that is an integer multiple of the sample period (*To* = *NTs*) only the fundamental harmonic appears in the frequency spectrum as is shown in Fig. 2. When the harmonic fundamental period is not equal to the length of observed signal block sequence spectral leakage occurs even in a case when only a one tone is given as is illustrated in Fig. 3.

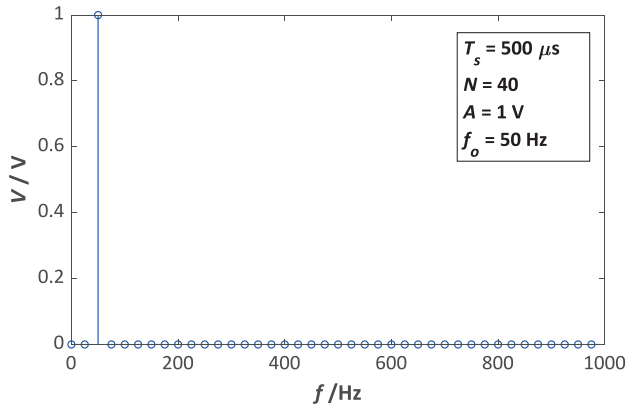


Fig 2.Signal spectrum without spectral leakage.

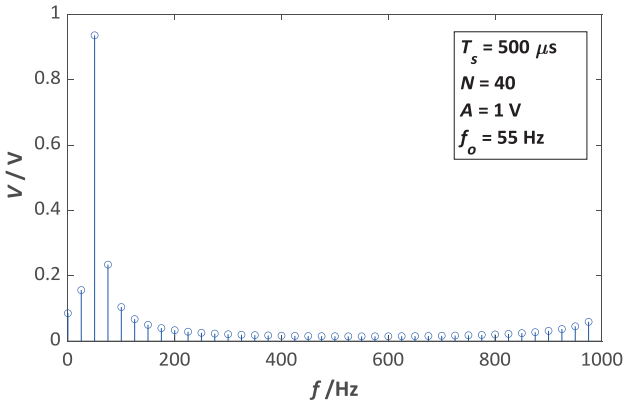


Fig 3. Signal spectrum with spectral leakage.



Antonijo Kunac, Marin Despalatović, Dario Šantić, Synchrophasors Determination Based on Interpolated FFT Algorithm, Journal of Energy, vol. 69 Number 1 (2020), p. 7–12

**Interpolation algorithm**

If the length of window does not contain an integer number of samples, i.e. it is not equal to the voltage fundamental period, leakage occurs. Because of that, the main tone of the signal is located between two consecutive DFT bins. For a such case, interpolation algorithms are used to obtain accurate magnitude and frequency value of the fundamental harmonic. In literature one can find a variety of interpolation formulas that can be used to derive the actual signal frequency from such a spectrum. The only requirement is that there is only a one frequency component in the observed band.

The simplest interpolation technique is to fit the parabola through three points and search for its maximum. The parabola equation used to estimate voltage magnitude is defined as follows

$$|V(\lambda)| = c\lambda^2 + b\lambda + a \tag{11}$$

where $\lambda$ is the intermediate variable in auxiliary coordinate system used to determine the exact frequency of the fundamental harmonic. To determine parabolic coefficients (*a*, *b*, *c*), system of three equations with three unknowns must be solved

$$\begin{bmatrix} 1 & \lambda & \lambda^2 \\ 1 & \lambda & \lambda^2 \\ 1 & \lambda & \lambda^2 \end{bmatrix} \begin{bmatrix} a \\ b \\ c \end{bmatrix} = \begin{bmatrix} |V[k_m - 1]| \\ |V[k_m]| \\ |V[k_m + 1]| \end{bmatrix} \tag{12}$$

where *km* is the sample index of the DFT's spectrum characterized by the magnitude |*V*[*km*]| of the middle frequency bin as is designated in Fig. 4. |*V*[*km*–1]| is the neighboring tone on the left side, while |*V*[*km*+1]| is the neighboring tone on the right side.

Square matrix on the left side of (12) takes the simplest form if the auxiliary ordinate ($\lambda$ = 0) passes through the middle frequency bin (*km*) and becomes

$$J = \begin{bmatrix} 1 & -1 & 1 \\ 1 & 0 & 0 \\ 1 & 1 & 1 \end{bmatrix} \tag{13}$$

To obtain solution of (12) one should calculate the inverse matrix of (13)

$$J^{-1} = \begin{bmatrix} 0 & 1 & 0 \\ -0.5 & 0 & 0.5 \\ 0.5 & -1 & 0.5 \end{bmatrix} \tag{14}$$

after which determination of parabola coefficients is straight forward

$$\begin{aligned} a &= |V[k_m]| \\ b &= 0.5 \cdot |V[k_m + 1]| - 0.5 \cdot |V[k_m - 1]| \\ c &= 0.5 \cdot |V[k_m - 1]| + 0.5 \cdot |V[k_m + 1]| - |V[k_m]| \end{aligned} \tag{15}$$

The maximum of the parabola (11) can be founded when its first derivative equals zero

$$2c\lambda_m + b = 0 \tag{16}$$

where fractional term

$$\lambda_m = \frac{|V[k_m - 1]| - |V[k_m + 1]|}{2 \cdot \left(|V[k_m - 1]| - 2|V[k_m]| + |V[k_m + 1]|\right)} \tag{17}$$

must satisfy $|\lambda m| < 1$. Once fractional term is known the maximum of the parabola is found for sample

$$k_{peak} = k_m + \lambda_m \tag{18}$$

as is illustrated in Fig. 4.

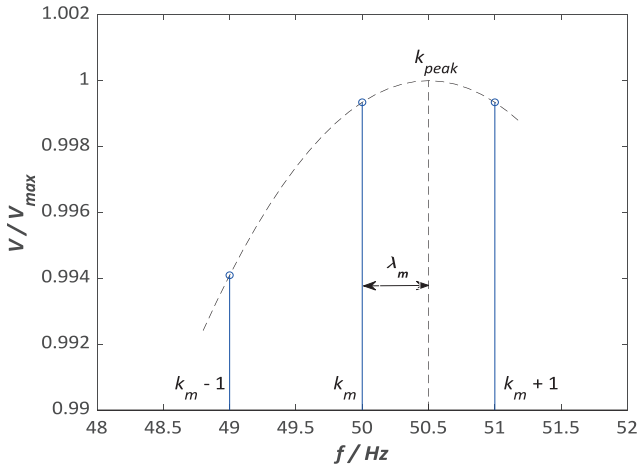


Fig 4. Illustration of parabola interpolation algorithm.

If we assume that duration of observed signal block sequence is equal to 40 ms, the DFT frequency resolution equals 25 Hz. This results with 25, 50 and 75 Hz bins on the frequency axis. Since interesting component of grid voltage is usually in vicinity of 50 Hz there is no need to count FFT at all points except in, for instance, 49, 50 and 51 Hz bins as is shown in Fig. 4. Instead of using a one second duration of signal block sequence to obtain frequency resolution of 1 Hz one can use the following convolution expression

$$V_M = \sum_{n=0}^{N-1} v[n] \cdot \mathrm{e}^{-\mathrm{j}\frac{2\pi M}{N}n} \tag{19}$$

to obtain corresponding frequency bins where *M* = {49, 50, 51}. The main advantage of (19) in comparison to DFT calculation is a shorter signal processing time since only three bins need to be processed and the length of block sequence needs to be at least 20 ms.

**Windowing technique**

To avoid consequences of spectral leakage and to improve accuracy of voltage magnitude and frequency estimated values a windowing technique is utilized [3], [7], [8]. Instead of (10), DFT spectrum of observed data block may be computed using a preselected windowing function as follows

$$V[k] = \frac{1}{B} \sum_{n=0}^{N-1} v[n] \cdot w[n] \cdot \mathrm{e}^{-\mathrm{j}\frac{2\pi k}{N}n} \tag{20}$$

where *w*[*n*] is usually the discrete Hanning windowing function that is used to extract a portion of the infinite length original sequence, and *B* is the DFT's normalization factor

$$B = \sum_{n=0}^{N-1} w[n] \tag{21}$$

It is important to note that fractional correction term $\lambda m$ is more accurate when windowing technique is applied. However, authors' focus is on how to find the correction term for determining the "accurate" frequency of the fundamental spectrum tone using computationally the most effective algorithm, which rectangular window is in comparison to Hanning window. This approach gives satisfactory accuracy and responsiveness as will be shown later in the paper.

# DESCRIPTION OF MODEL

Performance analysis of estimation algorithms has been carried out in MATLAB/Simulink environment by xPC Target model shown in Fig. 7 [11]. Presented model enables user to perform pure simulations on local (Host) computer as well as to perform rapid prototyping, i.e. hardware-in-the-loop testing on remote (Target) computer equipped with I/O hardware units. The mode of operation depends entirely on position of the two manual switches shown in Fig. 7.

The model consists of three parts. The first part (middle of Fig. 7.) comprises of setpoint magnitude and frequency generator in accordance with

(4)-(9). The main task of this part is to generate cosine and sine reference signals with arbitrary magnitude and frequency that acts as a rough approximation of the actual situation in the real power grid. At the same time these signals are also connected with analog output (D/A) block so they can be monitored as process variables by independent third-party measurement equipment. When manual switch is in "Simulation only" position these signals serve as inputs to estimation algorithm. Since reference signals are a priori known this mode of operation serves for theoretical accuracy and responsivity evaluation.

The second part (top of Fig. 7.) encompasses hardware analog input (A/D) block with offset and gain blocks for tuning accuracy in combination with blocks for transformation of two line-to-line voltages (*Uac*, *Ubc*) into $\alpha\beta$ variables, i.e. complex signal [9]. Manual switch position "Calibration" determines independent calibration procedure while position "Measurement" determines direct grid voltage syncrophasor measurements.

Finally, the third part (bottom of Fig. 7.) encompasses estimation algorithm. After generating a complex signal that represents transformed $\alpha\beta$ variables of three-phase voltage system, independently of switch position "Simulation only" or "Calibration/Measurement", three convolution sums for 49, 50 and 51 Hz are calculated. As can be seen for optimal deployment regarding computation and memory requirements it is preferable to implement convolution sum (19) in recursive form as is shown in Fig. 5.

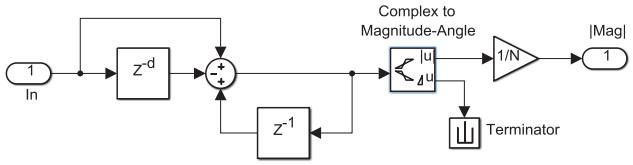


Fig. 5 Recursive model of convolution sum (19), delay d = N.

# SIMULATION RESULTS

Validity of previously described model as well as interpolation algorithms has been confirmed by numerous simulations under various grid operating conditions. Representative response on how estimated frequency tracks setpoint frequency is shown in Fig. 6.

To quantify quality of frequency estimation error the following expression is used

$$\Delta f = \left(f_{est} / f_{set} - 1\right) \times 100\,\% \tag{25}$$

where *fest* is the estimated frequency value, and *fset* is the frequency setpoint.

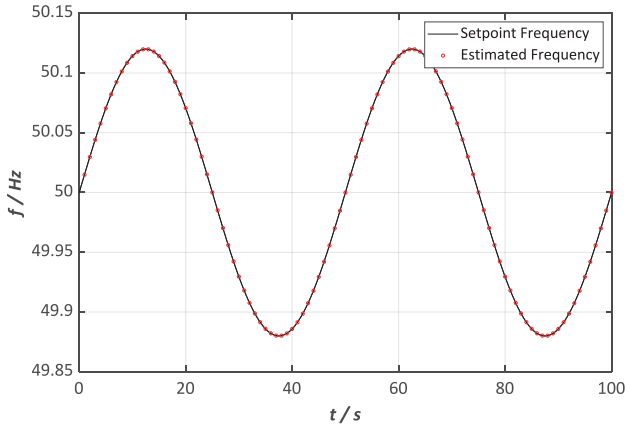


Fig. 6 Comparison of setpoint and estimated frequency for ΔF = 0.12 Hz and (Ω/2π) = 20 mHz

To demonstrate interpolation algorithm (17) and (18) effectiveness, the maximum absolute value of estimation error versus angular modulation frequency in (5) is observed. Obviously, estimation error rises as modulation frequency rises, and according to Fig. 8 this dependency is linear. As can be seen for modulation frequency of 2 Hz expected estimation error is less than 0.03 %. One should bear in mind that maximum value of grid voltage modulation frequency most of the time is less than 20 mHz, i.e. two orders of magnitude lower value. Thus, it may be concluded that presented estimation procedure is very accurate. The same is also valid for the interpolation algorithm based on windowing technique but computation time is longer while expected estimation error is less than the one shown in Fig. 8, i.e. the slope of line is lower.

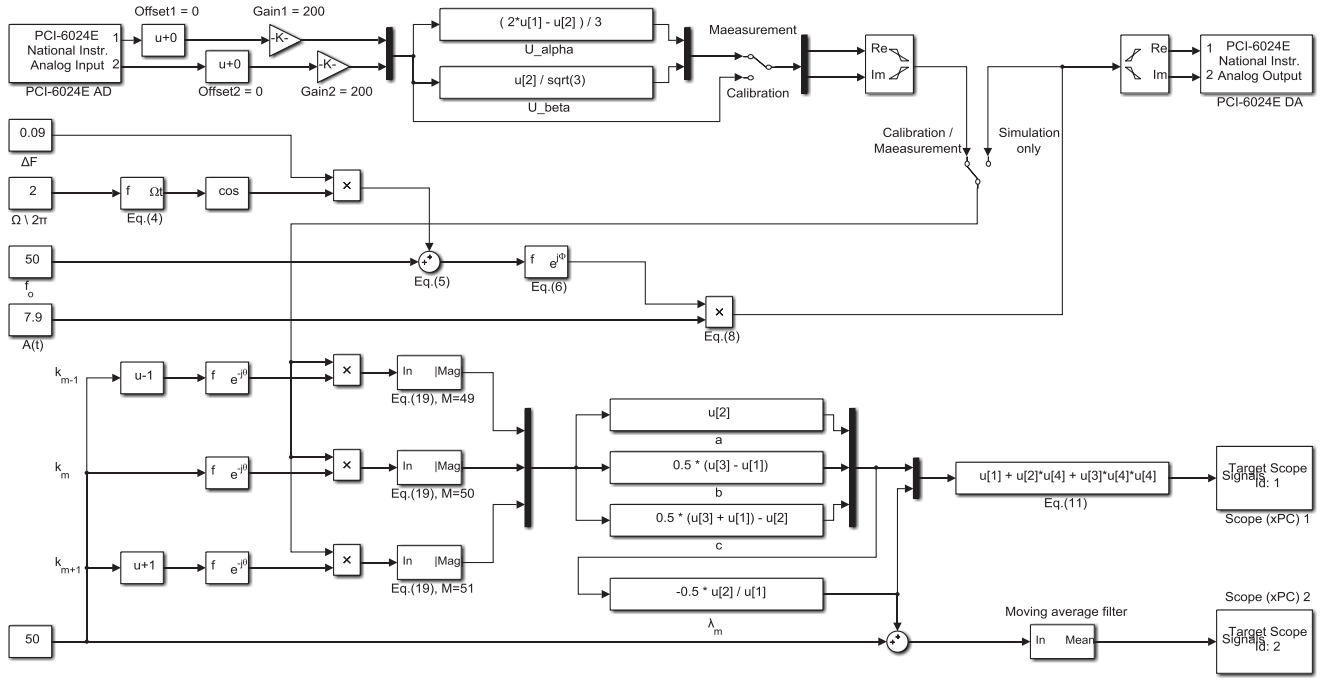


Fig. 7 xPC Target simulation model for determination of synchrophasors in MATLAB/Simulink.

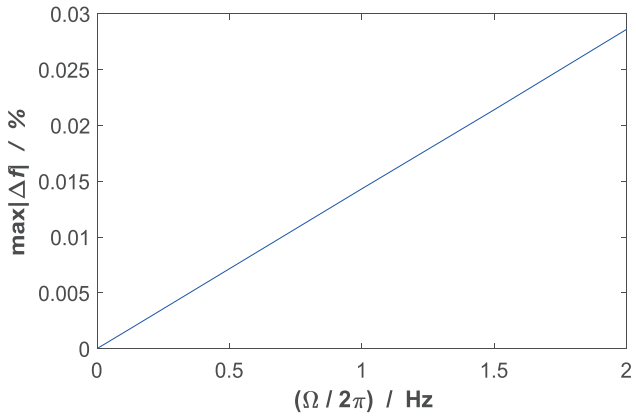


Fig. 8 Maximum estimation error versus modulation frequency.

# EXPERIMENTAL SETUP

The main part of the experimental setup is xPC Target platform in MATLAB/Simulink environment which enables rapid hardware-in-the-loop prototyping at affordable price-to-performance ratio. Laboratory testbed for grid voltage synchrophasor measurement is shown in Fig. 9. The standalone xPC Target computer showing real-time voltage monitoring is shown on the left side of the photography while on the right side is the Host PC showing xPC Target model on the middle screen and oscilloscope software on the right screen. For interaction with outside world 12-bit National Instruments' I/O data acquisition board PCI-6024E, located within desktop Target PC, is used. Since analog inputs' voltage measurement range are ±10 V a two 25 MHz bandwidth Pico Technology's TA057 differential probes were used for grid voltage measurement. For voltage and frequency calibration purposes independent measuring equipment consisting of Hewlett Packard's 3457A digital multimeter in combination with TiePie's HandyScope HS5 digital USB oscilloscope were used.

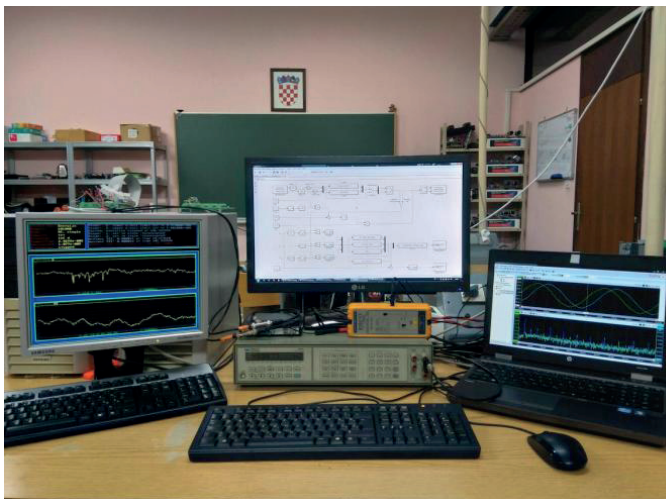

Fig. 9 Laboratory setup for grid voltage synchrophasor monitoring.

# EXPERIMENTAL RESULTS

Prior to recording grid voltage measurements calibration of laboratory setup was performed. As a first stage, internal calibration procedure was carried out in order to verify estimation algorithm accuracy and compensate for D/A and A/D offsets and gains. This is done simply by putting the left manual switch to "Calibration" position and the right switch in Fig. 7 to "Calibration/Measurement" position, and directly connecting analog outputs with corresponding analog inputs. At the same time multimeter and oscilloscope are also connected in parallel with board's I/O. Steady-state voltage waveforms of test signals during testbed calibration procedure are shown in Fig. 10. Response to dynamic frequency setpoint change obtained from standalone xPC Target system is shown in Fig. 11 which validates effectiveness of proposed estimation algorithm.

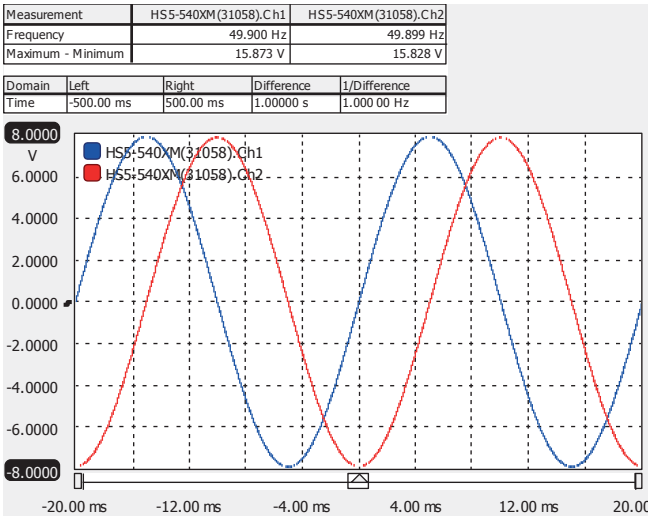


FDig. 10 Waveforms of test signals during testbed calibration procedure.

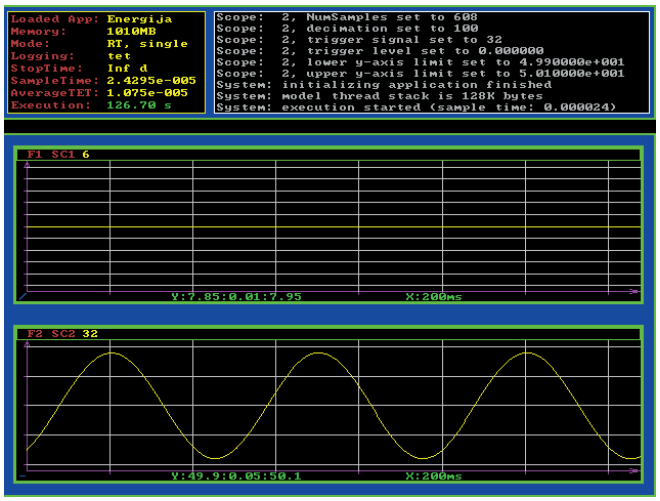


Fig. 11 Online monitoring of synchrophasor during calibration procedure for ΔF = 0.09 Hz and (Ω/2π) = 2 Hz.

In the second stage, after physically disconnecting analog inputs and outputs, external calibration procedure was carried out using programmable function generator under known conditions. For this purpose, the same USB oscilloscope is used since it is equipped with arbitrary waveform generator. Again, these measurements served as additional confirmation of calibration procedure.

After tuning offsets and gains steady-state voltage accuracy of 0.1 % of full-scale range and 1 mHz frequency accuracy were achieved. It should be emphasized that during transients estimated frequency value lags setpoint value by 10 ms, i.e. *N*/2 samples.

In order to encompass grid voltage measurement range separately calibrated differential probes with gains equal to 200 are connected to corresponding analog inputs. Steady- state waveforms of the line-to-line grid voltages during laboratory experiments are shown in Fig. 12. One can see that actual measured voltages can be unbalanced, and their frequency spectrums have higher harmonics besides the fundamental one. It should be pointed out that shown line-to-line voltages are deliberately chosen in a such a way to apply following $\alpha\beta$ transformation formulas [9]

$$u_\alpha = \frac{2}{3}u_{ac} - \frac{1}{3}u_{bc} \tag{22}$$

$$u_\beta = \frac{\sqrt{3}}{3}u_{bc}$$

while the zero-sequence voltage is always equal to zero.



Antonijo Kunac, Marin Despalatović, Dario Šantić, Synchrophasors Determination Based on Interpolated FFT Algorithm, Journal of Energy, vol. 69 Number 1 (2020), p. 7–12

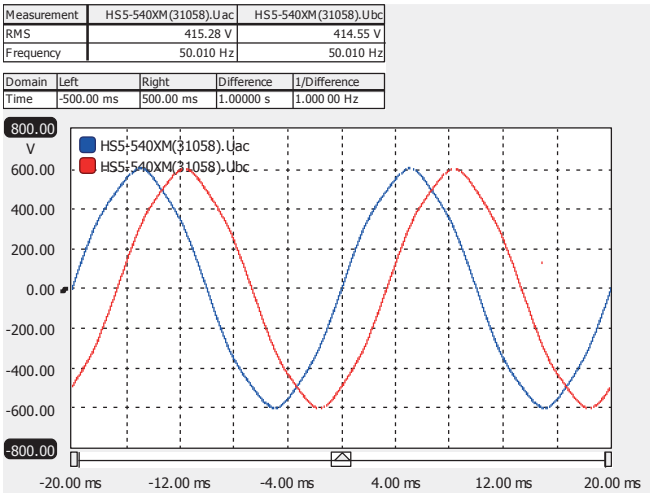


Fig. 12 Grid voltage waveforms during laboratory experiments.

Fig. 13 shows online monitoring of the grid voltage synchrophasor in FESB laboratory during 240 s interval. Due to presence of the grid voltage higher harmonics as well as to magnitude asymmetry, estimated frequency value besides steady-state dc value also has periodic ac value. A low pass moving average filter is used to eliminate the latter component (Fig. 7). This filter introduces additional lagging into estimation process equal to 10 ms, which aggregates in total to the period of the fundamental harmonic, i.e. to *N* samples.

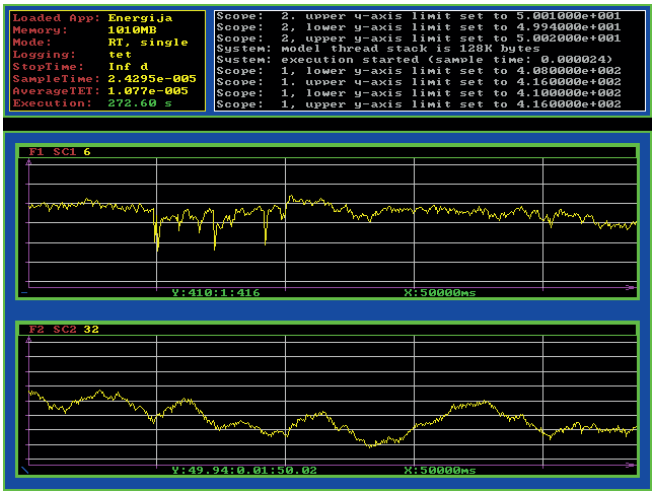


Fig. 13 Grid voltage synchrophasor online monitoring in FESB laboratory.

Note that the grid voltage magnitude ac component is significantly lower in comparison to the steady-state value. Thus, for the sake of simplicity the magnitude low-pass filter is omitted in Fig. 7.

Finally, representative response in Fig. 13 is selected as it shows a part of 7-minute interval where average grid frequency was approximately 49.97 Hz, i.e. it deviates 30 mHz from the rated value. Future work will involve inclusion of additional voltage statistics into the real-time monitoring system to ease analysis.

# CONCLUSION

This paper presents a procedure for monitoring syncrophasor of the fundamental voltage harmonic based on the IpDFT algorithm. Simulation analysis performed in MATLAB/Simulink demonstrate accuracy and responsivity of the algorithm given in the paper. In addition, calibration procedure performed using programmable function generator under known conditions as well as experimental analysis of grid voltage has also been carried out. The main advantage of implemented convolution sum technique realized in recursive form in comparison to classic DFT algorithms is speed and memory optimization. This study has been carried out in order to validate described measurement system for the monitoring of transients during island operation of a "small" local power electric system. Deployment of the presented algorithm to FPGA as well as introduction of a new functionalities as part of developing PQ monitoring system for field tests will be included in future work.

# ACKNOWLEDGMENT

This paper is fully supported by Croatian Science Foundation under the project Metrological infrastructure for smart grid IP-2014-09-8826.

# REFERENCES

[1] Q. Guo, and R. Gan, "An Arbitary-Resampling-based synchrophasor measurement algorithm in compliance with IEEE Std C37.118.1a-2014: Design, implementation, and validation", IEEE/PES Transmission and Distribution Conference and Exposition (T&D), July 2016.

[2] "IEEE Standard for Synchrophasor Measurments for Power Systems", IEEE Std C37.118.2-2011 (Revison of IEEE Std C37.118-2005), Dec. 2011.

[3] P. Romano, "DFT-based Synchrophasor Estimation Algorithms and their Integration in Advanced Phasor Measurement Units for the Real-time Monitoring of Active Distribution Networks ", PhD thesis, EPFL, Lausanne, 2016.

[4] P. Romano, and M. Paolone, "Enchanced Interpolated-DFT for Synchrophasor Estimation in FPGAs: Theory, Implementation, and Validation of a PMU Prototype", IEEE Transaction on Instrumentation and Measurement, vol. 63, pp. 2824-2836, Dec. 2014.

[5] P. Romano, M. Paolone, J. Arnold, and R. Piacentini, "An Interpolated-DFT Synchrophasor Estimation Algorithm and Its Implementation in an FPGA-based PMU Prototype", IEEE Power & Energy Society General Meeting, Nov. 2013.

[6] A.G. Phadke, and J.S.Thorp, "Synchronized Phasor Measurements and Their Applications", Springer Science+Business Media, LLC, 2008.

[7] G. Andria, M. Savino and A. Trotta: "Windows and interpolation algorithms to improve electrical measurement accuracy", IEEE Transactions on Instrumentation and Measurement, vol.38, pp. 856-863, 1989.

[8] M. Mandal, and A. Asif.: "Continuous and Discrete Time Signals and Systems", Cambridge University Press, New York, NY, 2007.

[9] A. M. Trzynadlowski: "Control of Induction Motors", Academic Press, San Diego, CA, 2001.

[10] D. G. Holmes, and T. A. Lipo: "Pulse Width Modulation for Power Converters", IEEE Press, Piscataway, NJ, 2003.

[11] "xPC Target User's Guide", The MathWorks Inc, Natick, MA, 2013.